

Supporting Information for

Plasmon modulated photothermoelectric photodetectors in silicon nanostripes

Weikang Liu[†], Wenqiang Wang[†], Zhiqiang Guan^{*†}, Hongxing Xu^{*†‡}

[†] School of Physics and Technology, Center for Nanoscience and Nanotechnology, and Key Laboratory of Artificial Micro- and Nano-structures of Ministry of Education, Wuhan University, Wuhan 430072, China

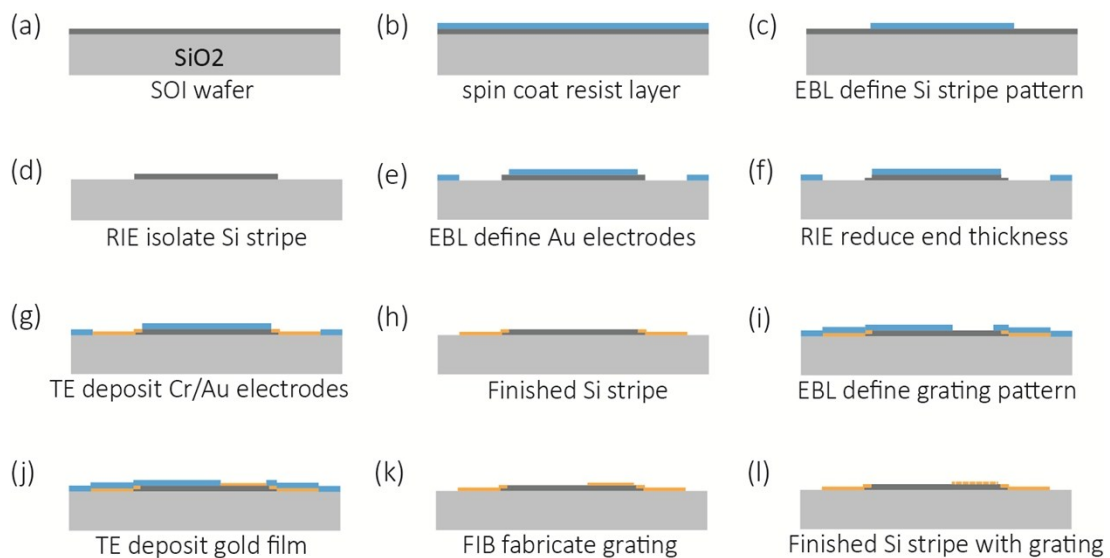
E-mail: zhiqiang.guan@whu.edu.cn, hxxu@whu.edu.cn

[‡] The Institute for Advanced Studies, Wuhan University, Wuhan 430072, China

1. Detailed fabrication process

Here we present a detailed fabrication process that is not included in main text. In preparation, large-area alignment marks are formed on the SOI wafer by ultraviolet exposure and thermal evaporation, then cut into small slices of 1 cm^2 and rinsed in acetone, alcohol, and pure water for lift-off. After drying the substrate using nitrogen, we spin-coat a 450 nm PMMA resist layer (4000 rpm, 1 min; AR-P 672.06, 950 K, AllRESIT PMMA) on the substrate, and bake the sample on a $150\text{ }^\circ\text{C}$ hot plate for 3 minutes. We define the Si stripe pattern by electron beam lithography (EBL, 20 kV, $220\text{ }\mu\text{C}/\text{cm}^2$, Raith eLINE Plus). The sample is developed in the developing solution (AR 600-56 for 1 min, IPA for 30 s) to keep the resist on the Si stripe and expose the excess part. Reactive ion etching (RIE, SF_6 , 35 s) is used to etch the excess Si, then

the sample is rinsed in acetone to remove the resist. We have obtained a bare Si stripe on the SiO_2 substrate (Figure 1d). In the step to make the electrode, EBL under the same experimental conditions is performed to define the electrode region. After development, RIE (SF_6 , 18 s) is used to reduce the thickness of the Si terminal to 80 nm, followed by thermal evaporation of a metal electrode (Cr/Au, 5 nm/180 nm, deposition rate: 0.4 A/s). The sample is lifted-off in acetone and rinsed in alcohol, followed by pure water, then we have the finished Si stripe with the electrode. In the final step, we make the nanograting structure on one side of the Si stripe. The nanograting is defined by EBL with the same experimental conditions, after development, 5 nm Cr and 105 nm Au are deposited followed by the lift-off process. Focused ion beam (FEI Versa 3D, 39 pA, 35 s) is used to mill the pattern of the nanoslits (25 nm slit width, 350 nm period) on the deposited film, resulting in the prepared sample (Figure 1l).



2. Oblique dark-field study of nanograting with 350 nm pitch

In the early experiments, in order to verify the rationality of the simulation results, we studied the spectra of the grating structure under oblique incident dark field. Compared with the reflection spectrum, the excitation angle of the oblique dark field is very fixed, and the experimental result is less affected by stray light. This method is very suitable for verifying simulation conditions. The experimental setup can be found in the supporting information of reference¹. Figure 2a is a SEM image of the device. The overlap rectangle in the image is the structure of the 350 nm grating on the SOI, same as in the main text. From the enlarged SEM image in Figure 2c, a well-controlled narrow-slit grating structure can be seen. Figure 2b is a CCD image of the device in experiment, and a vivid yellow color can be seen. The measured spectrum is shown in Figure 2d, and the simulation of the same structure is in Figure 2e. We find that the simulation is in good agreement with experimental result, which proves the calculation method is suitable for our structure.

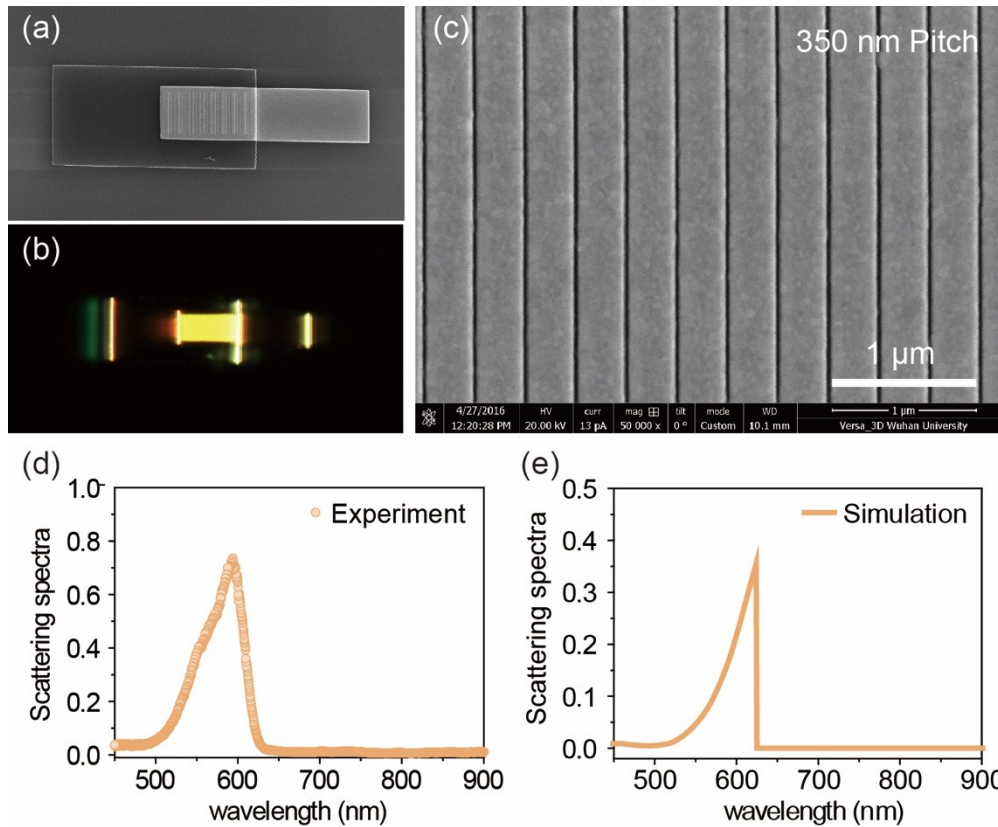


Figure 2. (a) SEM image of the sample. (b) Dark field image of the sample under oblique incident condition. (c) Enlarged SEM image, a well-controlled narrow slits grating structure (350 nm period) can be seen. (d), (e) The corresponding spectra obtained in measurement and simulation.

3. Comparison of the absorption in Si w/o nanograting

This section is a study of the enhancement effect of the narrow slits nanograting. For the nanograting structure and bare silicon, we calculate the electric field and absorption distribution at the 884 nm resonant peak by FDTD simulation (Figure 3a,b,c,d). The enhancement in the nanograting structure can be seen, when compared with the bare silicon. The plasmon resonance produces a standing wave waveguide mode inside the Si layer. In Figure 3e, we integrate the absorption of the Si layer to study the enhancement of the overall absorption at different wavelengths. The red line

is the absorption spectrum of the bare silicon, which decreases from around 750 nm, the black line represents the nanograting sample with enhancement at 653 nm and 884 nm. From the spectra, the nanograting provides 10 times the absorption enhancement compared with the absorption in the bare silicon layer. The simulated result at 884 nm reflects the photocurrent enhancement at 850 nm in the experiment.

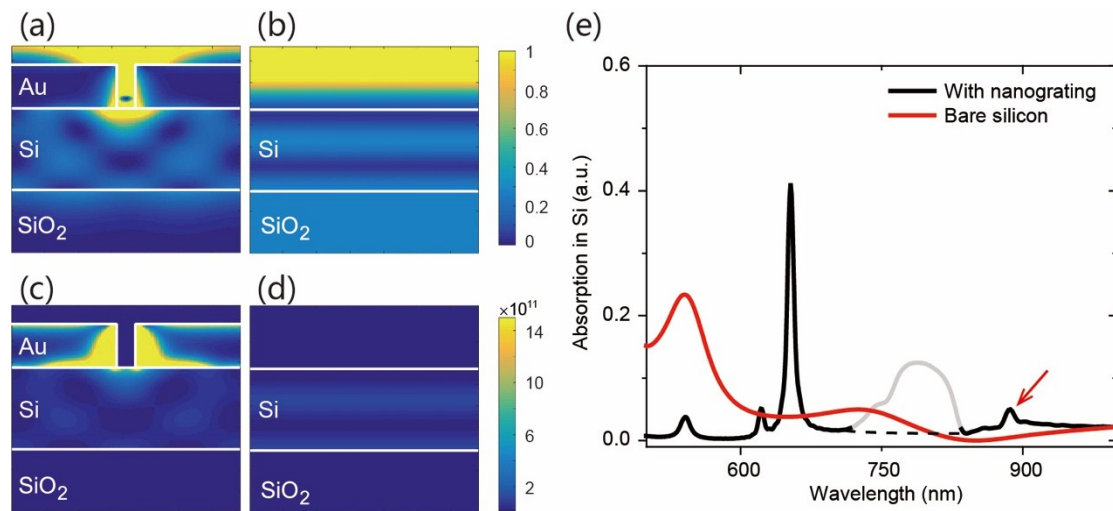


Figure 3. (a), (b) Electric field distribution in the structure w/o the nanograting calculated by the FDTD simulation. (c), (d) Absorption distribution in the structure w/o the nanograting. (e) Absorption spectra inside the Si layer in the bare silicon stripe and in the hybrid structure integrated with a nanograting. The peak at 884 nm corresponds to the 850 nm peak in the experimentally measured photocurrent enhancement. The redshift can also be observed in the reflection dispersion spectrum.

4. Wide-field photodetection under halogen lamp illumination

As described in the main text, our device also has wide-field detection capabilities because of the asymmetric structure. Figure 4a shows a CCD image of the device under halogen illumination. Figure 4b is the IV curve of the device measured in dark

and under the lamp illumination. The change of the photoconductivity can be observed from the IV curve, but the temperature difference between two ends of the device is small, so the IV curve still pass through the zero point. We measured the photovoltage of the device. When we increased the intensity of the illumination step by step, we found that the photovoltage continuously stepped up. The asymmetric structure causes the photovoltage to be negative, consistent with the data for photovoltage scanning with a focused laser. We have achieved a photovoltage responsivity of more than 16 mV/mW (Figure 4c).

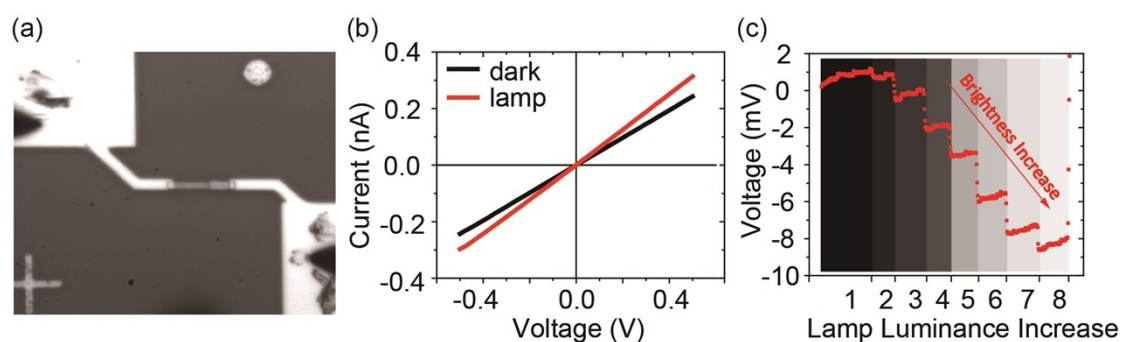


Figure 4. (a) CCD image of our measured sample. Halogen lamp provides the wide-field illumination. (b) I-V curve of the device measured in dark and under the lamp illumination. (c) Measured photovoltage versus different lamp luminance. A photovoltage responsivity of more than 16 mV/mW is detected.

Reference

1. Zheng, D.; Zhang, S. P.; Deng, Q.; Kang, M.; Nordlander, P.; Xu, H. X., Manipulating Coherent Plasmon-Exciton Interaction in a Single Silver Nanorod on Monolayer WSe₂. *Nano Lett* **2017**, *17* (6), 3809-3814.